Journal of the Air & Waste Management Association

Radical precursors and related species from traffic as observed and modeled at an urban highway junction

Bernhard Rappenglück [a] , Graciela Lubertino [b] , Sergio Alvarez [a] , Julia Golovko [a] , Beata
Czader [a] & Luis Ackermann [a]

[a] Department of Earth and Atmospheric Sciences , University of Houston , Houston , TX , USA

[b] Houston-Galveston Area Council , Houston , TX , USA
Accepted author version posted online: 18 Jul 2013.Published online: 16 Oct 2013.

PLEASE SCROLL DOWN FOR ARTICLE

TECHNICAL PAPER

Radical precursors and related species from traffic as observed and modeled at an urban highway junction

Bernhard Rappenglück,[1,*] Graciela Lubertino,[2] Sergio Alvarez,[1] Julia Golovko,[1] Beata Czader,[1] and Luis Ackermann[1]

[1]Department of Earth and Atmospheric Sciences, University of Houston, Houston, TX, USA
[2]Houston-Galveston Area Council, Houston, TX, USA
*Please address correspondence to: Bernhard Rappenglück, Department of Earth and Atmospheric Sciences, University of Houston, 4800 Calhoun Rd., Houston, TX 77204, USA; e-mail: brappenglueck@uh.edu

Nitrous acid (HONO) and formaldehyde (HCHO) are important precursors for radicals and are believed to favor ozone formation significantly. Traffic emission data for both compounds are scarce and mostly outdated. A better knowledge of today's HCHO and HONO emissions related to traffic is needed to refine air quality models. Here the authors report results from continuous ambient air measurements taken at a highway junction in Houston, Texas, from July 15 to October 15, 2009. The observational data were compared with emission estimates from currently available mobile emission models (MOBILE6; MOVES [MOtor Vehicle Emission Simulator]). Observations indicated a molar carbon monoxide (CO) versus nitrogen oxides (NO_x) ratio of 6.01 ± 0.15 ($r^2 = 0.91$), which is in agreement with other field studies. Both MOBILE6 and MOVES overestimate this emission ratio by 92% and 24%, respectively. For HCHO/CO, an overall slope of 3.14 ± 0.14 g HCHO/kg CO was observed. Whereas MOBILE6 largely underestimates this ratio by 77%, MOVES calculates somewhat higher HCHO/CO ratios (1.87) than MOBILE6, but is still significantly lower than the observed ratio. MOVES shows high HCHO/CO ratios during the early morning hours due to heavy-duty diesel off-network emissions. The differences of the modeled CO/NO_x and HCHO/CO ratios are largely due to higher NO_x and HCHO emissions in MOVES (30% and 57%, respectively, increased from MOBILE6 for 2009), as CO emissions were about the same in both models. The observed $HONO/NO_x$ emission ratio is around 0.017 ± 0.0009 kg HONO/kg NO_x which is twice as high as in MOVES. The observed NO_2/NO_x emission ratio is around 0.16 ± 0.01 kg NO_2/kg NO_x, which is a bit more than 50% higher than in MOVES. MOVES overestimates the CO/CO_2 emission ratio by a factor of 3 compared with the observations, which is 0.0033 ± 0.0002 kg CO/kg CO_2. This as well as CO/NO_x overestimation is coming from light-duty gasoline vehicles.

Implications: Nitrous acid (HONO) and formaldehyde (HCHO) are important precursors for radicals that ultimately contribute to ozone formation. There still exist uncertainties in emission sources of HONO and HCHO and thus regional air quality modeling still tend to underestimate concentrations of free radicals in the atmosphere. This paper demonstrates that the latest U.S. Environmental Protection Agency (EPA) traffic emission model MOVES still shows significant deviations from observed emission ratios, in particular underestimation of HCHO/CO and $HONO/NO_x$ ratios. Improving the performance of MOVES may improve regional air quality modeling.

Introduction

The hydroxyl radical (•OH) is the most important oxidant in the atmosphere and controls the atmospheric lifetimes of most trace gases. •OH is largely produced in photolysis processes of ozone (O_3), formaldehyde (HCHO), and nitrous acid (HONO) (e.g., Elshorbany et al., 2009; Mao et al., 2010). Minor •OH sources are associated with photolysis of hydrogen peroxide (H_2O_2) and nitryl chloride ($ClNO_2$) and ozonolysis of alkenes, the latter being an important nighttime source for •OH.

•OH initiates oxidation reactions with nitrogen oxides (NO_x; $NO_x = NO + NO_2$), carbon monoxide (CO), and anthropogenic and biogenic volatile organic compounds (VOCs). These reactions form peroxy radicals (RO_2), which in turn will cause the conversion of nitrogen monoxide (NO) to nitrogen dioxide (NO_2) and subsequently the formation of O_3. Within the degradation of VOC also carbonyls will be formed, which either may be photolyzed (e.g., HCHO) or oxidized by •OH and finally contribute to the formation of peroxycarboxylic nitric anhydrides (PANs). Loss mechanisms for •OH involve reactions between peroxy radicals leading to H_2O_2 and organic peroxides, e.g., methylhydroperoxide (MHP) and hydroxylmethylhydroperoxide (HMHP), and reactions with NO_2 leading to nitric acid (HNO_3) and PANs.

An analysis using the Community Multiscale Air Quality (CMAQ) model 4.71 (Byun and Schere, 2006) for Houston, Texas (Figure 1), shows that although photolysis of ozone is an
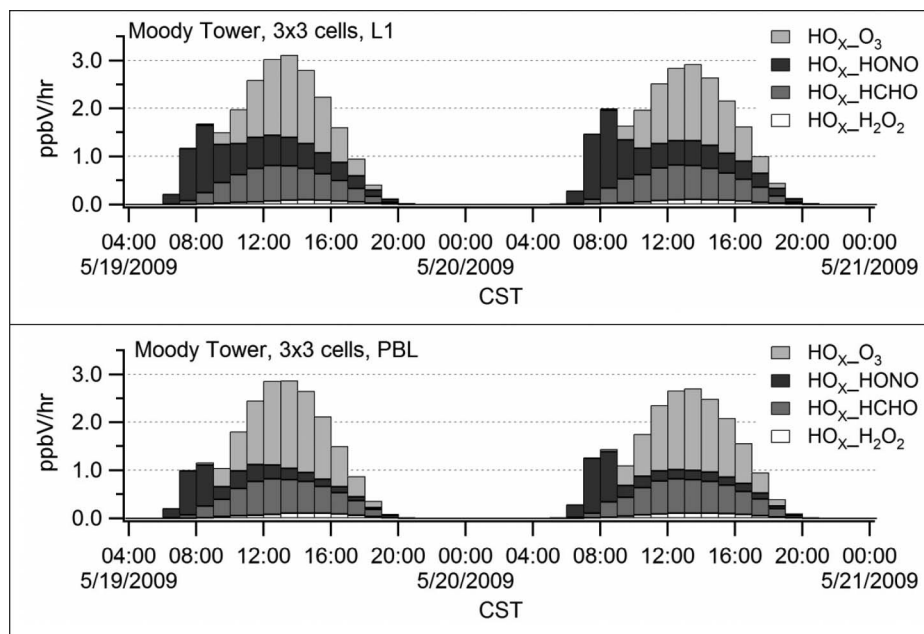
Figure 1. CMAQ modeling of contribution of O_3, HONO, HCHO, and H_2O_2 to hourly HO_x formation for the Moody Tower site in Houston, Texas, on May 19–20, 2009. Above: data extracted from the first model layer; below: data averaged up to the height of the planetary boundary layer.

important source for •OH around noon and in the afternoon hours, HCHO may contribute most to •OH formation during late morning hours, and HONO is a very efficient source for •OH formation during early morning hours (Czader et al., 2013).

Although HCHO may be produced through reactions of alkenes with •OH, it can also be formed from ozonolysis of terminal olefins or emitted primarily from incomplete combustion in either mobile or stationary sources (Zweidinger et al., 1988; Altshuller, 1993; Chen et al., 2004; Dasgupta et al., 2005). These latter processes represent net •OH sources. Traffic-related emission ratios of HCHO/CO were found to be around 1.3–1.4 ppt$_v$ HCHO/1 ppb$_v$ CO in earlier studies (Anderson et al., 1996), whereas more recent studies report higher values (Rappenglück et al., 2005, 2010).

HONO can be emitted primarily from various combustion processes (Kirchstetter et al., 1996; Kurtenbach et al., 2001) and emissions from traffic can significantly contribute to observed HONO levels. For example, Sarwar et al. (2008) found that direct emissions contributed ~14% to the HONO budget in their model, based on emission ratios on literature values (Kirchstetter et al., 1996; Kurtenbach et al., 2001). The results indicated exhaust emission ratios of HONO to NO_x in the range of 0.3–0.8% (Kirchstetter et al., 1996; Kurtenbach et al., 2001; Kleffmann et al., 2003). Different emission ratios may reflect a different composition of the car fleet. The first two measurements were obtained in tunnel studies. However, tunnel measurements may be biased due to the restrictions for specific vehicles, e.g., heavy-duty vehicles (Kirchstetter et al., 1996, McGaughey et al., 2004).

So far, only scarce traffic emission data are available that include both compounds. In particular for HONO, traffic-related data were obtained more than a decade ago. A better knowledge of today's HCHO and HONO emissions related to traffic is needed to further refine and validate air quality models such as CMAQ as

well as to predict/simulate impact of these emissions on air quality. Here we will report results from roadside measurements performed in Houston, Texas, an urban area, which has been classified as in nonattainment for the 1-hr and the 8-hr ozone standards by the U.S. Environmental Protection Agency (EPA) and has been the focus of some recent urban air quality studies (e.g., Parrish et al., 2009; Lefer and Rappenglück, 2010; Olaguer et al., 2013).

Table 1 provides information about daily emissions of NO_x, VOC, and CO in Harris County, which encompasses most of the Houston metropolitan area. Due to a very limited public transportation system, significant mobile emissions occur. On-road emissions constitute an important source for NO_x and CO and account for 48.5% (NO_x) and 51.2% (CO) of the overall NO_x and CO emissions in Harris County. For VOC emissions, point and area sources play a major role in Houston due to its large industrial, in particular petrochemical, facilities, located in the Houston Ship Channel to the East of the Houston's urbanized area (e.g., Leuchner and Rappenglück, 2010). Still, according to Table 1, VOC traffic emissions are non-negligible. In addition, the fraction of traffic-related VOCs of the overall VOC emissions reaches its diurnal maximum during the early morning rush hours (Leuchner and Rappenglück, 2010).

In this paper, real-world observational roadside data related to traffic emissions are compared with emission estimates from currently available mobile emission models, i.e., MOBILE6 versus MOVES (MOtor Vehicle Emission Simulator). Although there have been some comparisons between MOBILE6 and MOVES with regard to differences in model performance (Vallamsundar et al., 2011; Kota et al., 2012), only a few recent publications compare results from MOBILE6 and MOVES with observational data. Fujita et al. (2012) studied CO/NO_x and non-methane hydrocarbon (NMHC)/NO_x molar ratios in a traffic tunnel, whereas Wallace et al. (2012) compared modeled

Table 1. Daily emissions of NO_x, VOC, and CO in Harris County in short tons per day (tpd)

Source Category	NO_x (tpd)	VOC (tpd)	CO (tpd)	$\%NO_x$	%VOC	%CO	CO/NO_x
Points[a]	51.5	89.7	52.6	16.6	24.2	4.2	1.0
Non-road[b]	51.9	34.8	438.9	16.7	9.4	35.4	8.5
On-road[c]	150.8	63.3	634.8	48.5	17.1	51.2	4.2
Off-road[d]	39.3	5	45.9	12.6	1.3	3.7	1.2
Area[b]	17.5	177.9	66.9	5.6	48.0	5.4	3.8
Total	311.0	370.7	1239.1	100.0	100.0	100.0	4.0

Notes: [a]From 2009 STARS (State of Texas Air Reporting System; http://www.tceq.texas.gov/airquality/point-source-ei/psei.html). [b]From 2008 TEX-N Non-road; sources include construction equipment, recreational boating lawn care, and logging (Texas nonroad; http://www.tceq.texas.gov/airquality/airmod/overview/am_ei.html#nonroad) model and TexAER (Texas Air Emissions Repository; http://www.tceq.texas.gov/airquality/areasource/TexAER.html). [c]From 2008 TTI MOVES. [d]From 2006 baseline for the HGB SIP (Houston-Galveston-Brazoria State Implementation Plan); off-road sources include aircraft, locomotive, drilling rigs, and marine engines.

CO/NO_x ratios in MOBILE6 and MOVES with observations at a regional monitoring site. However, to our understanding, some limitations in the work of Wallace et al. (2012) exist because they applied MOBILE6 and MOVES for different modeling dates. To our knowledge, no comparison and validation with roadside measurements for other ratios related to traffic emissions such as NO_2/NO_x, CO/CO_2, and in particular ratios involving radical precursors such as HCHO/CO and $HONO/NO_x$ have been carried out so far. Contrary to MOBILE6, MOVES includes modeling of HONO and CO_2, which is a major addition. In this paper, we focus on compound ratios because these tend to be preserved in emission plumes, whereas compound concentrations would be prone to dilution (e.g., Bishop and Stedman, 1996; Klemp et al., 2002; Franco et al., 2013). Because our measurements site was very close to the traffic emission sources and strict data screening was performed, we assume that chemical processes affecting specific compounds were kept minimal. Considering multiple compound ratios allowed investigating potential biases in the emission models for a given compound. For instance, if NO_2/NO_x would had been modeled correctly, but was based on wrong emissions for both NO_2 and NO_x, this would have shown up in $HONO/NO_x$, unless HONO emission also had been based on wrong assumption. This in turn could be proved by HONO/CO and CO/NO_x.

Methods

Experimental data

During the time period July 15–October 15, 2009, continuous ambient air measurements were taken at the Highway Junction I-59 South/610 located in the Galleria, Houston, area (Figure 2), which is located about 10 km to the west of the Houston downtown area. This highway junction has the highest traffic loads of all highway junctions in Houston, with about 400,000 vehicles daily for 2009 (Texas Department of Transportation [TxDOT], 2009a), of which 5–10% were heavy-duty diesel vehicles (see Table 4). A mobile measurement shelter was set up close to a pumping station maintained by TxDOT. This pumping station is used by TxDOT in emergency only, e.g., when flooding occurs, which did not happen during the field campaign. Table 2 lists

selected variables and their measurement techniques at this site, which include HCHO, HONO, CO, $NO/NO_2/NO_x$, PANs, and meteorological parameters. This location was completely surrounded by highway lanes, ramps, and other roads and impacted by traffic emissions regardless of the wind direction. Because the measurements of speciated PANs had the longest measurement interval (10 min), all the data were merged to a 10-min interval database. In order to determine traffic-related emissions only, a subset of 10-min averaged data was used that met the following conditions:

(1) Weekdays
(2) Rush hour time 4:00–8:00 a.m. Central Standard Time (CST)
(3) Global radiation <10 Wm^{-2}
(4) PANs <50 ppt_v
(5) No precipitation
(6) Relative humidity (RH) $>80\%$

Morning rush hour times were used because they represent one prominent peak in the diurnal variation of the traffic emission strength as described by the term VMT (vehicle miles traveled), as shown in Figure 4. Contrary to the afternoon rush hour, the morning rush hour times also coincide with lowest boundary layer height (e.g., Rappenglück et al., 2008) associated with a minimum of vertical mixing. During the afternoon, the boundary layer is well mixed and most likely impacted by the preceding morning residual layer (e.g., Morris et al., 2010).

Conditions 1–3 made sure that only rush hour times with negligible radiation were included to avoid any bias introduced by photochemical reactions. Condition 4 was applied to discriminate freshly emitted air masses from photochemically aged air masses. Although conditions 1–4 already yielded high correlation coefficients for various relationships, e.g., CO versus NO_x or HCHO versus CO, the inclusion of conditions 5–6 led to significant increase of r^2 for relationships including HONO, e.g., HONO versus NO_x and HONO versus CO, which points to better representation of combustion-related emission processes for HONO in these cases.

The above prerequisites are very strict conditions. For instance, condition 3 limited further significantly the available data sets for rush hour times because sunrise often occurred
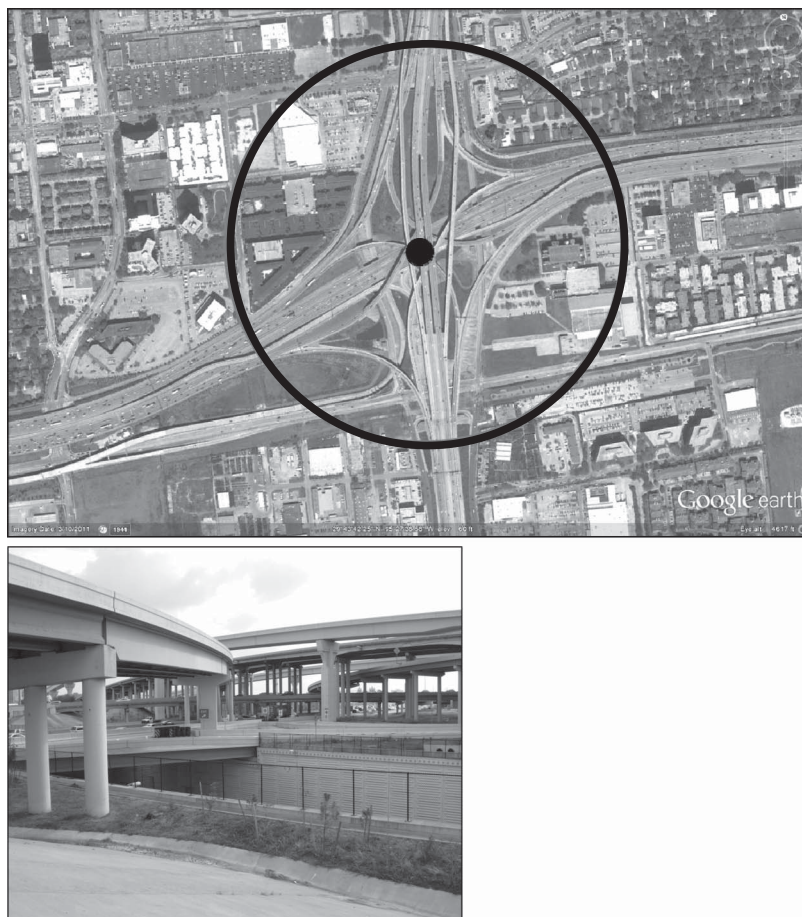
Figure 2. Above: Highway Junction I-59 South/610 in the Houston area. The black dot indicates the center of the traffic emission modeling area; the circle around the dot has a radius of 1000 feet and indicates the outer border of the traffic emission modeling area. Below: Partial view of the Highway junction shows where the measurements were taken.

Table 2. List of measured variables and measurement techniques at the Galleria site

Parameter	Method	Instrument	Detection Limit	Uncertainty
HONO	Long path absorption photometer	LOPAP 03	1–2 ppt_v	$\pm 10\%$
NO	Chemiluminescence	TE 42i TL	50 ppt_v	$\pm 7\%$
NO_2	Chemiluminescence/photolytic conversion	TE 42i TL/BLC	50 ppt_v	$\pm 12\%$
HCHO	Hantzsch/fluorescence	AL4021	60 ppt_v	$\pm 10\%$
CO	Gas filter correlation	TE 48i TLE	10 ppb_v	$\pm 5\%$
CO_2	Differential, nondispersive infrared absorption	LI-7000	1 ppm_v	$\pm 1\%$
Peroxycarboxylic nitric anhydrides (PANs)	Gas chromatography/electron capture detection (GC/ECD)	Modified Metcon GC/ECD	10 ppt_v	$\pm 10\%$
Wind speed	Sonic (WINDCAP)	Vaisala WXT510	0.1 m/sec	$\pm 2\%$
Wind direction	Sonic (WINDCAP)	Vaisala WXT510	$1°$	$\pm 2\%$
Temperature	Capacitive (THERMOCAP)	Vaisala WXT510	0.1 °C	± 0.3 °C
Relative Humidity	Capacitive (HUMICAP)	Vaisala WXT510	0.1%	$\pm 3\%$ (0–90%) $\pm 5\%$ (90–100%)
Rainfall	Acoustic (RAINCAP)	Vaisala WXT510	0.01 mm	$\pm 5\%$
Barometric pressure	Capacitive (BAROCAP)	Vaisala WXT510	0.1 hPa	± 0.5 hPa
Solar radiation	Pyranometer	Vaisala QMS 101	0.1 W/m^2	$<2\%$

Table 3. Statistical data for the Galleria site measurements (database: 10 min)

Parameter	HONO (ppt$_v$)	NO (ppb$_v$)	NO$_2$ (ppb$_v$)	NO$_x$ (ppb$_v$)	HCHO (ppb$_v$)	CO (ppb$_v$)	CO$_2$ (ppm$_v$)	PAN[a] (ppt$_v$)	PPN[b] (ppt$_v$)
Maximum	5185	137.9	64.3	161.7	16.9	1309	527.3	4148	859
Mean	615	9.3	13.4	22.9	2.8	262	407.8	306	28
Median	500	5.6	11.5	18.5	2.3	238	403.8	175	15

Notes: [a]Peroxyacetyl nitrate. [b]Peroxyproprionyl nitrate.

before 8:00 a.m. CST. Also, condition 4 is a very strict condition, keeping in mind the wide range of PANs values, as shown in Table 3. As a test for the validity of this approach, a correlation analysis of CO concentrations in ppb$_v$ versus NO$_x$ concentrations in ppb$_v$ was performed first. The results of this analysis are shown in Figure 3. The data set displays strong relationship of CO versus NO$_x$ ($r^2 = 0.91$), with a slope of 6.01 ± 0.15 ppb$_v$ CO/1 ppb$_v$ NO$_x$. This is in very good agreement with Parrish et al. (2009) for rush hour times in selected cities. Due to the high value for r^2, we assume that any bias of the observed CO/NO$_x$ due to chemical processes and/or superimposed by other sources is negligible. We thus consider our data screening to be representative of traffic emissions. CO/NO$_x$ ratios have decreased in the United States over the last years due to a slow decrease of CO emissions slightly compensated by an increase in NO$_x$ emissions (Parrish et al., 2009). Our observed molar CO/NO$_x$ ratio is of similar magnitude as that found by Luke et al. (2010), who determined a range of 5.8 ± 0.9 for the CO/NO$_x$ ratio at the Moody Tower on the campus of the University of Houston at 70 m above ground level. Because the Moody Tower site is not directly impacted by traffic sources, this may explain that the uncertainty related to their determination of the CO/NO$_x$ ratio is significantly larger ($r^2 = 0.81$) than the one reported in our paper.

Emission modeling

Before discussing details of our emission modeling approach, we briefly summarize the main differences between MOBILE6 and MOVES:

- MOBILE6 had not been updated since 2003, and as a consequence it is using very old data assumptions. MOVES is based on more recent information (EPA, 2013), although not all Tier 2 engines data have been analyzed by EPA yet, and as a consequence not totally incorporated.
- New data have shown that extended idling and deterioration of heavy-duty diesel vehicles were underestimated in the past. As a consequence, MOVES shows a large increase in NO$_x$ and particulate matter (PM) emissions versus MOBILE6.
- For light-duty gasoline vehicles, the emission reductions from NO$_x$ and VOC coming from the inspection and maintenance program are much less in MOVES than in MOBILE6. The difference between the two models only grows as a user models later evaluation years, due to different assumptions for future NO$_x$ and VOC emission reductions (EPA, 2013).
- CO$_2$ emissions are speed, temperature, and fuel dependent in MOVES, unlike in MOBILE6.
- MOVES calculates "off-network" emissions, which are emissions mainly coming from parking lots, in a separate category.
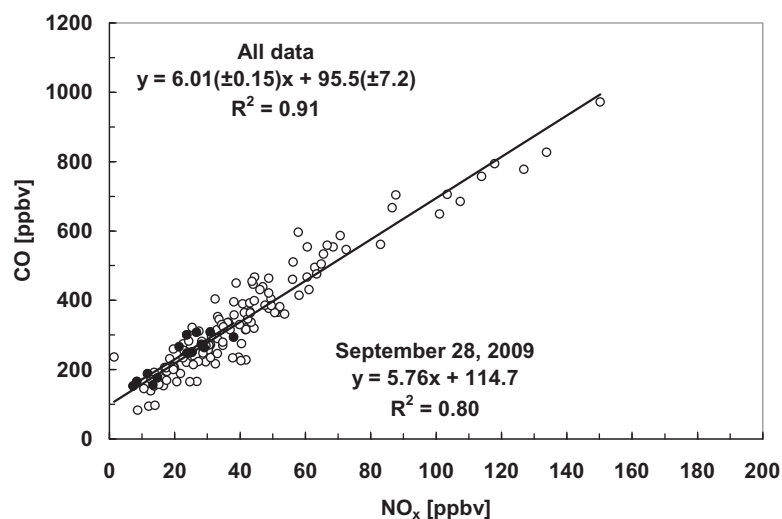

Figure 3. Correlation of CO versus NO$_x$ as obtained at the Galleria site during July 15–October 15, 2009, for morning rush hour times. Black dots indicate the data for September 28, 2009. Data screened as described in the text. Values based in brackets are based on 95% confidence level.

These emissions include engine starts, evaporative, and idling. On the contrary, MOBILE6 lumps all these emissions together in the on-road category.

In this paper, we used the traffic emission models MOBILE6 and MOVES for the area of the measurement site for September 28, 2009, as an exemplary day. This day was chosen because the experimental data showed maximum data availability for one given day based on the data screening approach described above in the section "Experimental Data." An hourly link-based calculation was performed, including all the emissions coming from all the links around 1000 feet radii around the intersection (see Figure 2). Following is the explanation of the different inputs that went into each model.

MOBILE6. The link-based emissions were calculated using the Texas Transportation Institute (TTI) suite of programs (TxDOT, 2009b), which combines the emission factors from the latest version of MOBILE6.2 (EPA, 2003) with the VMT. The VMT was calculated using EMME2 (Equilibre Multimodel, Multimodel, Equilibrium 2) as the travel demand model for the 2009 Houston road network, which was validated using road specific traffic counts by the Federal Highway Administration (FHWA) Highway Performance Monitoring System (HPMS).

The following parameters were chosen to calculate the hourly Harris County emission factors for on-road:

(1) Observed meteorology (hourly temperature and relative humidity; daily averaged atmospheric pressure) at the Galleria site for the model day: September 28, 2009
(2) 2009 local registration distribution
(3) 2009 local diesel fractions
(4) 2009 local VMT per hour
(5) Local inspection and maintenance program
(6) Antitampering program
(7) Reformulated gasoline

Then, the emission factors were adjusted, using the TTI suite of programs, for the Texas Low Emission Diesel and the Motorcycle Rule (Houston-Galveston Area Council [H-GAC], 2009). The final link-based emission calculations were done using the adjusted emission factors, the 2009 VMT mix (distribution of VMT according to vehicle type and fuel), and the

2009 hourly link VMT and speeds activity estimates calculated with EMME2. The output is link-level emissions per hour by vehicle type in grams.

The emission calculations were performed for the following pollutants: NO_x, VOC, CO, and formaldehyde. It was decided not to perform the calculation for CO_2 because MOBILE6 has a very simple capability to calculate CO_2 emission factors and is mainly based on fuel economy, and unlike other pollutants, these CO_2 emission factors are independent of temperature, speed, fuel content, or effects due to the inspection and maintenance program. As a consequence, these CO_2 emission factor estimates should only be used to model areas and time periods that are large enough to assume that the variation of these parameters do not have a significant impact.

All these calculations were done considering the local 2009 diesel/gasoline split on the arterial and freeway facility types, as shown in Table 4. The splits were calculated using 2009 TxDOT traffic counts for each facility type. Figure 4 shows the diurnal weekday variation of VMT for the Galleria site study area for 2009. It clearly reflects the different time periods as defined in Table 4; in particular, it shows the two rush hour periods with

Table 4. Diesel-gasoline split on the arterial and freeway facility types used as input for MOBILE6 and MOVES calculations

Time of Day_Facility Type	Diesel Percentage	Gasoline Percentage
AM_Arterial	7%	93%
AM_Freeway	5%	95%
MD_Arterial	11%	89%
MD_Freeway	9%	91%
PM_Arterial	6%	94%
PM_Freeway	5%	95%
OV_Arterial	7%	93%
OV_Freeway	7%	93%

Notes: AM = morning peak, from 6:00 to 9:00 a.m. CST; MD = mid-day period, from 9:01 a.m. to 3:00 pm CST; PM = afternoon peak, from 3:01 to 7:00 p.m. CST; OV = overnight period, from 7:01 p.m. to 6:00 a.m. CST.
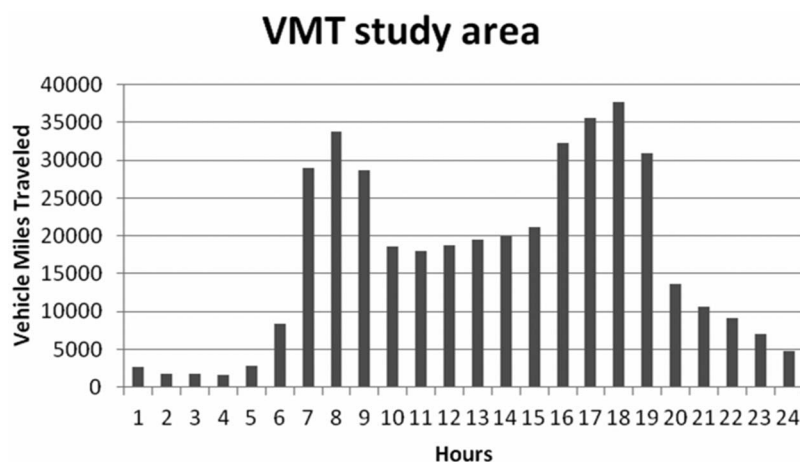

Figure 4. Diurnal variation of VMT for the Galleria site study area September 28, 2009.

VMT in the range of 30,000–35,000 per hour and the mid-day period, which has about 60% of the rush hour VMT. During the overnight periods, VMT is usually in the 2000–5000 range.

MOVES2010a and MOVES2010b.   The emissions were calculated using MOVES2010a (EPA, 2010a) as an emission factor model for the following pollutants: NO_x, CO, VOC, formaldehyde, CO_2 (atmospheric), NO, NO_2. Then, when MOVES2010b (EPA, 2012) became available, HONO was also calculated.

The link-based emissions were calculated using the "TTI Emission Inventory Estimation Utilities Using MOVES: MOVESUTL" (TxDOT, 2011), which combines the emission factors from MOVES with VMT. For this scenario, the same VMT data were utilized, as described in the previous section.

The following tables were used to enter local data into the MOVES County Data Manager to calculate the 2009 hourly Harris County emission factors for "on-road" and "off-network":
(1) Avgspeeddistribution—lists the average speed data specific to vehicle type, road type, and time of day.
(2) Dayvmtfraction—lists the daily VMT fractions according to day type, source type, road type, and month. Validated with local FHWA-HPMS data.
(3) Fuelformulation—lists properties of fuels from the Houston region.
(4) Fuelengfraction—lists the vehicle types with different types of fuels (represents the old diesel fractions on MOBILE6) from local, i.e., Harris County vehicle registration data collected by the Texas Commission on Environmental Quality (TCEQ).
(5) Fuelsupply—lists the market share for each fuel for the Houston region.
(6) Hourvmtfraction—lists the hourly VMT fractions according to the hour, source type, road type, and day type. Validated using FHWA-HPMS traffic counts.
(7) Hpmsvtypeyear—lists the year VMT for each source use type. Validated using FHW-HPMS traffic counts.
(8) Imcoverage—lists information regarding inspection and maintenance programs for the Houston region.
(9) Monthvmtfraction—lists monthly VMT fractions according to month type and source type.
(10) Roadtypedistribution—lists the distribution of vehicle miles traveled by road type. Validated with FHWA-HPMS traffic counts.
(11) Sourcetypeagedistribution—lists the distribution of vehicle counts by age from TCEQ Harris county vehicle registration data.
(12) Sourcetypeyear—lists the number of vehicles in geographic area per source type from TCEQ Harris County vehicle registration data.
(13) Zonemonthhour—lists hourly temperature, relative humidity, and daily averaged atmospheric pressure data as observed at the Galleria site for the modeling day, September 28, 2009.

Then the emission factors were adjusted, using the TTI utilities, for the Texas Low Emission Diesel and the Motorcycle Rule (H-GAC, 2009). For "on-road" and "off-network" sources, the emission calculations were done using the adjusted emission factors, the local 2009 source use type (SUT) mix, as shown in

Table 4, the off-network activity (vehicle population, source hours parked, starts, and extended idle hours), and the 2009 hourly link VMT and speeds activity estimates calculated with EMME2. The output is hourly link-level emissions by SUT–fuel type combination. Please note that for "on-road" emissions, only the links selected for the study area were used in the calculations. For "off-network" emission, the total county emissions were adjusted according to the ratio between the study area versus the county area.

Results and Discussion

Table 3 lists some statistical data about the field campaign measurements. It is worth to note that median values of HONO concentrations were at relatively high levels about 0.5 ppb_v, whereas median values concentrations of other predominantly primarily emitted compounds (NO_x, CO) showed some modest values. HONO maximum concentration values of about 5 ppb_v occurred in the early days of September 2009, coinciding with high ozone concentrations reported by the Houston Continuous Ambient Monitoring Station (CAMS) sites. The highest ozone mixing ratio on September 3, 2009, reached up to 157 ppb at Bayland Park (CAMS 53). On the same day, HCHO and PAN at the Galleria site reached maximum values.

Figure 5 displays the diurnal observational averages of PAN, HONO, CO, NO_x, HCHO, and global radiation. It can be seen that the concentrations of HONO and HCHO increase together with those of CO and NO_x during the morning rush hour, about 4:00–7:00 a.m. CST (see (I) in Figure 5). After 7:00 a.m. CST, still during the rush hour period, breakdown of the nocturnal boundary layer leads to a decrease of NO_x and CO concentrations. Both HCHO and HONO follow NO_x and CO in a similar way until about 7:00 a.m. CST. Then, HONO and HCHO show different behavior: whereas HONO still shows a trend similar to NO_x and CO, HCHO increases. The increase of HCHO is primarily due to photochemical formation of HCHO from VOCs, as global radiation starts to increase. Photochemical production is also indicated by the increase of PAN and the elevated PAN levels during the day (see (II) in Figure 5). Still, some fraction of ambient HCHO is also likely due to ongoing traffic emissions. As seen in (III) in Figure 5, sustained CO levels at around 300 ppb_v prevail during daytime and are higher than during nighttime, when lower planetary boundary height would favor accumulation of CO. Also, HONO stays at relatively high levels (about 600 ppt_v), although photochemical and consequently photolysis processes are high, as indicated by (II) in Figure 5. The high levels of HONO may likely be due to direct traffic emissions. Other potential formation pathways might be conversion of HNO_3 to HONO on primary organic aerosol (Ziemba et al., 2010) or heterogeneous formation from NO_2 (Kleffmann et al., 1998; Finlayson-Pitts et al., 2003; Czader et al., 2012).

The bottom plot in Figure 5 shows that the average HONO/NO_x ratio varies between 2% during the morning rush hour and up to 5% during nighttime hours. This is a range that is similar to values found elsewhere (Lammel and Cape, 1996; Elshorbany et al., 2009; Villena et al., 2011). The HONO/NO_x ratio shown in Figure 5 is primarily determined by emissions, removal processes, and transport of air masses that may contain different
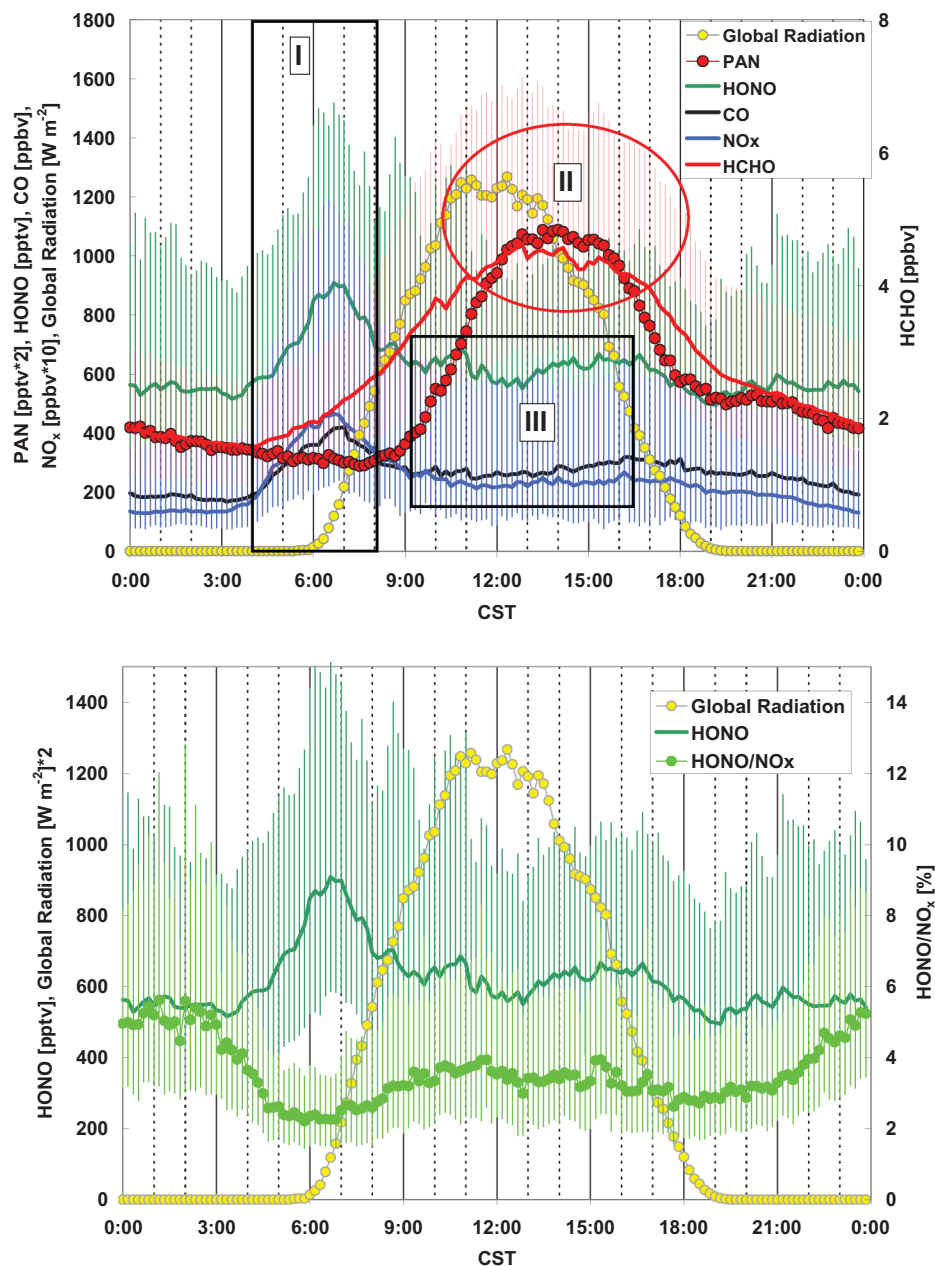
Figure 5. Above: Average diurnal variation of PAN, HONO, CO, NO_x, HCHO, and global radiation at the Galleria site during July 15–October 15, 2009. The numbers indicate the following sections: (I) morning rush hour, (II) photochemical processes, and (III) elevated levels throughout the day due to ongoing traffic. Below: Average diurnal variation of HONO, HONO/NO_x, and global radiation at the Galleria site during July 15–October 15, 2009. Bars indicate 1σ distribution of the observed data for any given time stamp.

amounts of NO_x and/or HONO. However, it is noteworthy that HONO/NO_x ratios during rush hour (about 2%) and around noontime (about ~3.5–4%) are slightly higher than in environments where higher NO_x mixing ratios were reported (e.g., Elshorbany et al., 2009; Villena et al., 2011).

Table 5 shows all the observed compound ratios obtained at the measuring site during July 15–October 15, 2009, for morning rush hour times and separately for September 28, 2009, morning rush hours, which is used for model comparison. Note: In order to compare the observational data with the emission ratio results calculated by the emission model, we used the

molecular weight of 46 for each individual reactive nitrogen compound, HONO, NO, NO_2, and NO_x, which is in compliance with EPA rules for the use of emission models (EPA, 2011).

According to Table 5, the experimental data for all days reflect an emission ratio of 3.67 $\pm$ 0.09 kg CO/kg NO_x. Table 5 also shows the experimental results for September 28, 2009, which was the day used for MOBILE6 and MOVES modeling. The results for September 28 are slightly lower, with 3.51 kg CO/kg NO_x. Figure 6 shows the CO/NO_x ratio simulated with MOBILE6 and MOVES. For the rush hour period, MOBILE6 significantly overestimates the CO/NO_x emission

Table 5. Observed compound ratios as obtained at the Galleria site during July 15–October 15, 2009, for morning rush hour times ("All Data") and for September 28, 2009, the data used for model comparison

Compounds	All Data		September 28, 2009	
	Slope (kg/kg)*	r^2	Slope (kg/kg)*	r^2
CO vs. NO_x	3.67 ($\pm$ 0.09)	0.91	3.51	0.80
HCHO vs. CO	3.14 ($\pm$ 0.14)	0.68	2.69	0.68
HONO vs. NO_x	0.017 ($\pm$ 0.0009)	0.75	0.016	0.88
HONO vs. CO	0.0046 ($\pm$ 0.0002)	0.75	0.0037	0.70
NO_2 vs. NO_x	0.16 ($\pm$ 0.01)	0.48	0.18	0.50
NO vs. NO_x	0.84 ($\pm$ 0.01)	0.96	0.82	0.95
CO vs. CO_2	0.0033 ($\pm$ 0.0002)	0.73	n/a	n/a

Notes: Standard deviation values, given in parentheses, are based on 95% confidence level. In order to compare the observational data with the emission ratio results calculated by the emission model, the molecular weight of 46 for HONO, NO, NO_2, and NO_x was used, which is in compliance with EPA rules for the use of emission models (EPA, 2011). *For HCHO versus CO, the ratio is given in g/kg.
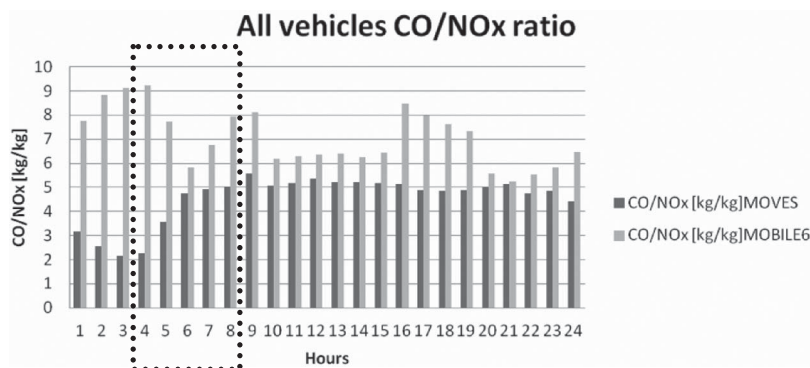
Figure 6. Diurnal variation of the CO/NO_x ratio for the Galleria study site for September 28, 2009, as calculated by MOBILE6 and MOVES. The average of the early morning hours is 4.56 kg of CO per kg of NO_x using MOVES, and 7.06 kg of CO per kg of NO_x using MOBILE6. The dash box indicates the hours used to take the average. Times are in CST.

ratio (7.06 kg CO/kg NO_x), whereas MOVES is getting closer to the observed values (4.56 kg CO/kg NO_x), but still about 30% higher than the observed values. The values we obtained from our analysis of MOBILE6 and MOVES are significantly lower, and thus also closer to the observed data, than the ones reported by Wallace et al. (2012). They are similar to CO/NO_x values obtained in California (Bishop et al., 2012). Figure 7 shows the CO/NO_x ratio for light-duty gasoline and heavy-duty diesel vehicles calculated using MOVES, which are 9.2 and 0.42, respectively, for the early morning hours (4:00–8:00 a.m. CST). The overall VMT split during this time period is 95% for light-duty gasoline vehicles and 5% for heavy-duty diesel vehicles. These results indicate that the MOVES CO/NO_x over-estimation is related to the overestimation of CO from light-duty gasoline vehicles.

Figures 8–11 display the modeling results for the radical precursors HCHO and HONO versus CO and HONO versus NO_x using MOBILE6 and MOVES. For HCHO/CO (Table 5), the observational data yield an overall slope of 3.14 $\pm$ 0.14 g HCHO/kg CO. On September 28, 2009, an emission ratio of 2.69 g HCHO/kg CO was determined. Figure 8 shows that

MOBILE6 largely underestimates this ratio, showing a HCHO/CO (g/kg) of 0.7 throughout the day. MOVES calculates higher HCHO/CO ratios than MOBILE6 for the same morning rush hour period, an average of 1.87 g of HCHO per kg of CO, but is still lower than the observed ratio. MOVES shows surprisingly high HCHO/CO ratios during the early morning hours due to heavy-duty diesel "off-network" emissions. The reasons for these large "off-network" emissions are idling and starting trucks. Heavy-duty diesel vehicles are known to be major sources for traffic-related HCHO emissions (Ban-Weiss et al., 2008). Accordingly, Figure 9 shows the HCHO/CO (g/kg) ratio for light-duty gasoline and heavy-duty diesel vehicles calculated using MOVES, which are 0.67 and 24.43, respectively, for the morning rush hour period.

The differences of the modeled CO/NO_x and HCHO/CO ratios between MOBILE6 and MOVES for the model year 2009 are due to higher NO_x emissions in MOVES (30% increased from MOBILE6) and higher HCHO emissions in MOVES (57% increased from MOBILE6); CO emissions were about the same in both models, as shown in Figure 10. These differences are mainly due to different model assumptions and
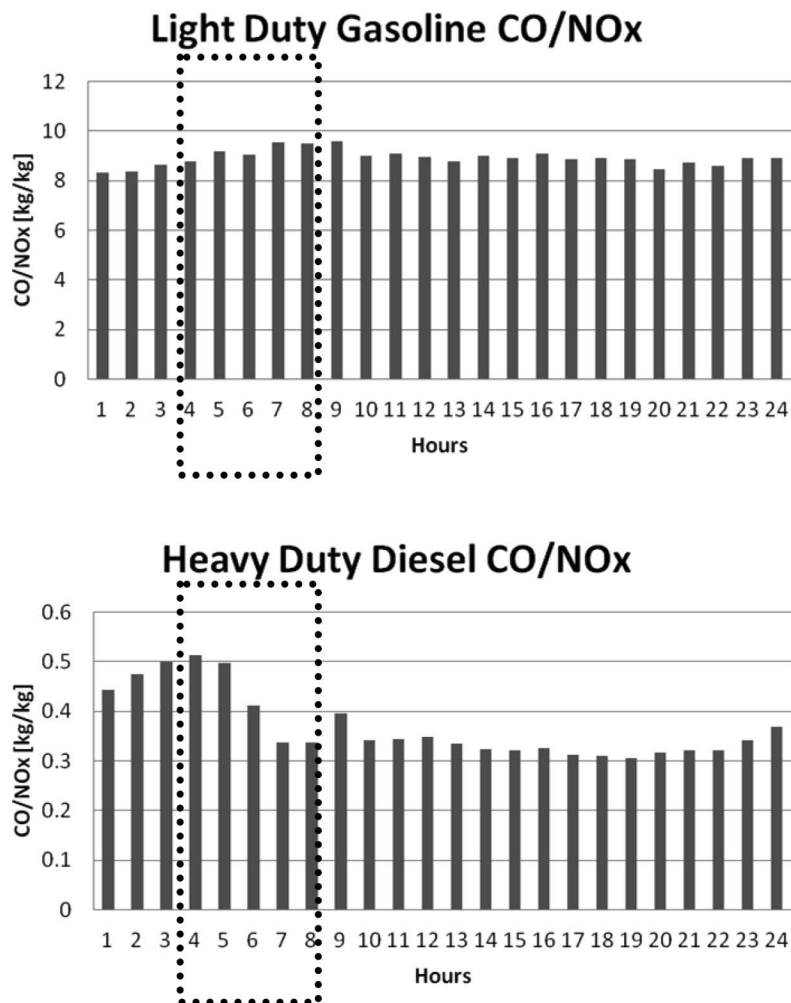
Figure 7. Diurnal variation of CO/NO$_x$ ratio for light-duty gasoline and heavy-duty diesel vehicles calculated using MOVES. The average of the early morning hours is 9.20 kg of CO per kg of NO$_x$ and 0.42 kg of CO per kg of NO$_x$, respectively. The dash box indicates the hours used to take the average. Times are in CST.
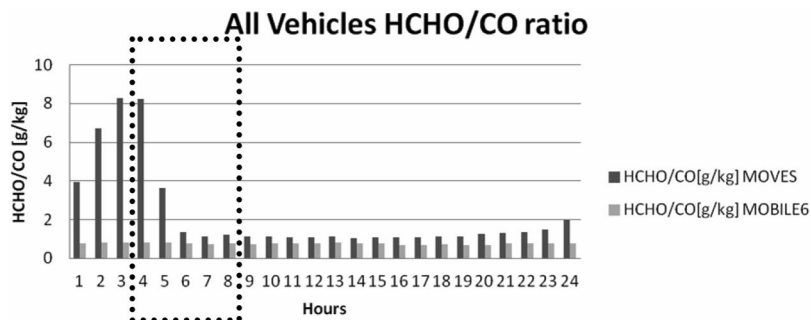

Figure 8. Diurnal variation of the HCHO/CO ratio for the Galleria study site for September 28, 2009, as calculated by MOBILE6 and MOVES. The average of the early morning hours is 1.87 g of HCHO per kg of CO using MOVES, and 0.7 g of HCHO per kg of CO using MOBILE6. The dash box indicates the hours used to take the average. Times are in CST.

the increased importance of off-network emissions due to extended idling and deterioration of heavy-duty diesel vehicles, as outlined before in the section "MOVES2010a and MOVES2010b."

Contrary to any previous traffic emission model, MOVES2010b is the first model that allows modeling HONO

emissions. MOVES calculations showed a HONO/NO$_x$ emission ratio of 0.008 kg HONO/kg NO$_x$ (plot not shown), constant throughout the day, which reflects results obtained in earlier tunnel studies (Kurtenbach et al., 2001). Table 5 shows the correlation analysis based on observational data during morning rush hour, which reflects the relative change ΔHONO versus
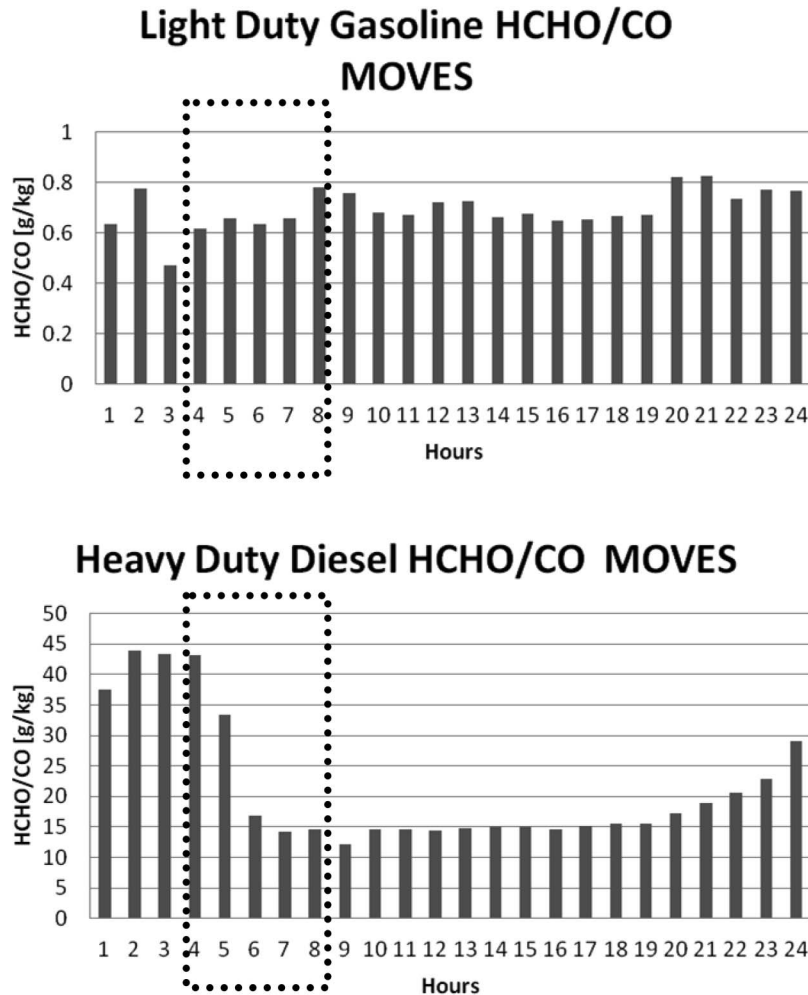
Light Duty Gasoline HCHO/CO MOVES

Heavy Duty Diesel HCHO/CO MOVES

Figure 9. Diurnal variation of HCHO/CO ratio for light-duty gasoline and heavy-duty diesel vehicles calculated using MOVES. The average of the early morning hours is 0.67 g of HCHO per kg of CO and 24.43 g of HCHO per kg of CO, respectively. The dash box indicates the hours used to take the average. Times are in CST.

ΔNO_x and can thus be interpreted as an emission ratio, contrary to Figure 5 that displays instantaneous $HONO/NO_x$ ratios. The observed $HONO/NO_x$ emission ratio (Table 5) is around 0.017 ± 0.009 kg $HONO$/kg NO_x, which is twice as high as in MOVES. A potential reason for the discrepancy between MOVES and the our observational data might be that previous tunnel studies did not include heavy-duty diesel vehicles (e.g., Kirchstetter et al., 1996) and/or that today's traffic fleet composition does not coincide with those studied about 15 yr ago. Also, the same $HONO/NO_x$ ratio is used throughout for all vehicle categories in MOVES, which may not necessarily be the case (Kurtenbach et al., 2001). Table 5 also includes an analysis of HONO versus CO. Using CO as a tracer for traffic emissions shows a very good correlation of HONO versus CO ($r^2 = 0.75$), with a slope of 0.0046 ± 0.0002 kg $HONO$/kg CO (and 0.0037 kg $HONO$/kg CO on September 28, 2009). The close correlation with combustion processes is also reflected in the correlation of HONO versus CO_2 ($r^2 = 0.66$; plot not shown). It is worth to note that the relationships of HONO versus CO and CO_2 are even better than HCHO versus CO ($r^2 = 0.68$) and CO_2 ($r^2 = 0.39$). Although it is obvious that due to the lower $HONO/NO_x$

emission ratios, MOVES will also likely calculate lower $HONO/$ CO emission ratios, as shown in Figure 11, the modeled ratio is 0.0021 kg $HONO$/kg CO for the early morning hours and thus significantly lower.

Table 5 displays the experimental results for the NO_2/NO_x emission ratio. In an earlier experimental study, which was done in 1997 and performed concurrently with traffic-related HONO emissions, a NO_2/NO_x emission ratio of about 5% was determined (Kurtenbach et al., 2001). In Figure 12, MOVES results for the rush hour time indicate a ratio of about 9.3% (0.093 kg of NO_2 per 1 kg of NO_x) for all vehicles, with an average of 9.2% and 10.6% for heavy-duty diesel and light-duty gasoline vehicles, respectively (not shown). The experimental data (as shown in Table 5) show even higher values (18% for September 28, 2009; 16% for all rush hour data). It might be possible that the observed NO_2 could have been produced through titration with O_3, whereas the air mass was brought to the analyzer. As the background O_3 might have been different for each individual observation, this could explain the scatter of the data and thus the modest value for r^2. In order to exclude any bias of the NO_2/NO_x ratio, potentially introduced by O_3 titration, we looked into NO/
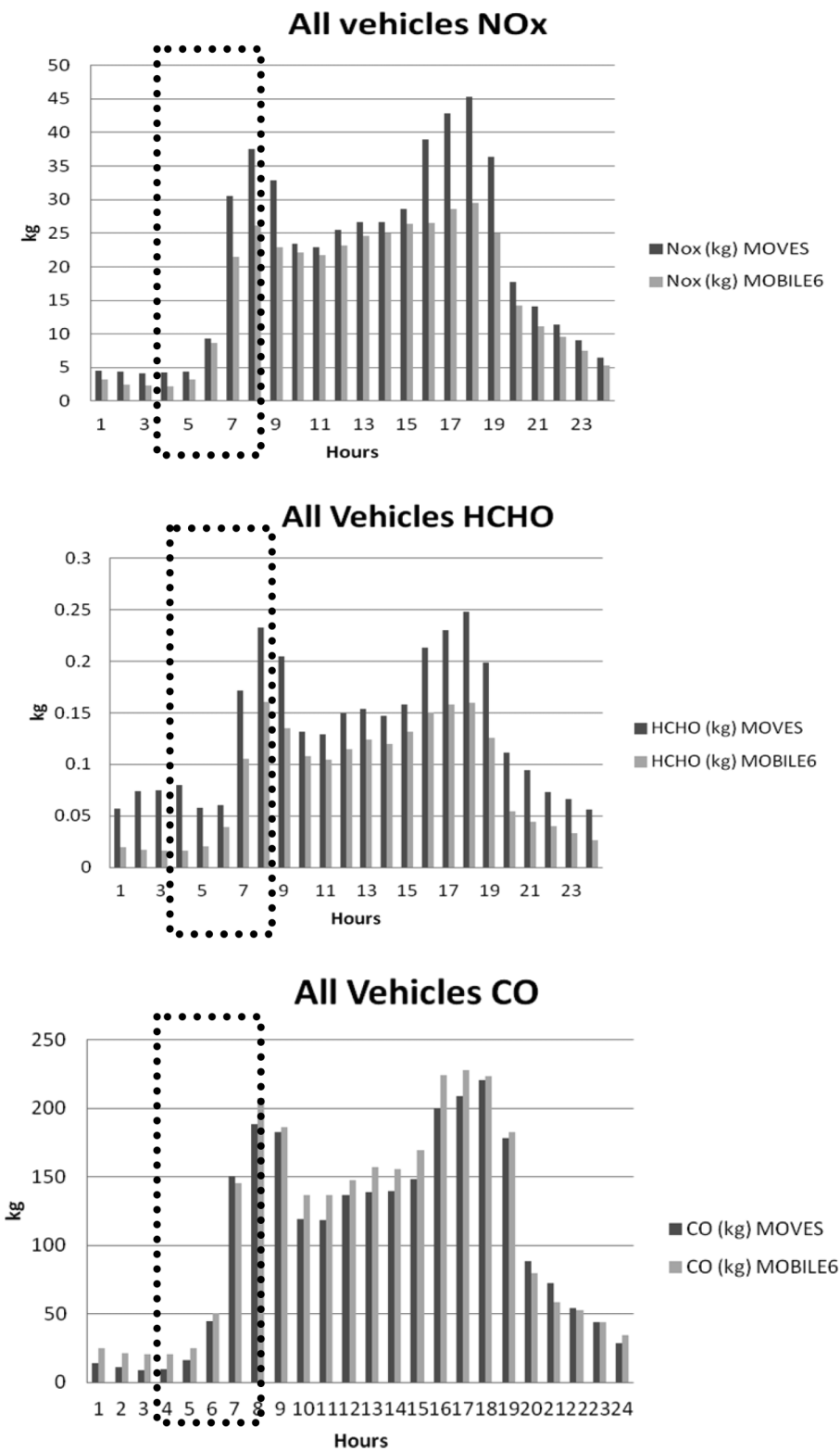
Figure 10. Diurnal variation of NO$_x$, HCHO, and CO emissions for all vehicles calculated with MOBILE6 and MOVES. The NO$_x$ average emission in the early morning hours is 17.22 kg using MOVES and 12.36 kg using MOBILE6. The HCHO average emission in the early morning hours is 0.12 kg using MOVES and 0.07 kg using MOBILE6. The CO average emission in the early morning hours is 81.65 kg using MOVES and 89.83 kg using MOBILE6. The dash box indicates the hours used to take the average. Times are in CST.
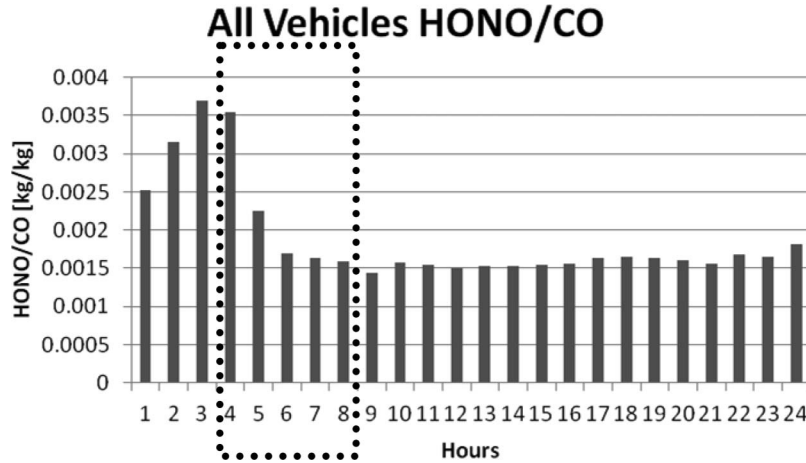
Figure 11. Diurnal variation of the HONO/CO ratio for the Galleria study site for September 28, 2009, as calculated by MOVES. The average of the early morning hours is 0.021 kg of HONO per kg of CO. The dash box indicates the hours used to take the average. Times are in CST.
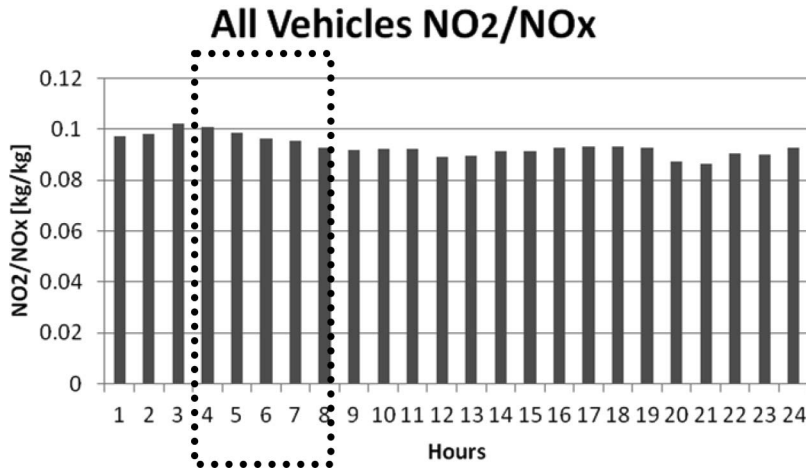

Figure 12. Diurnal variation of the NO_2/NO_x ratio for the Galleria study site for September 28, 2009, as calculated by MOVES. The average of the early morning hours is 0.093 kg of NO_2 per kg of NO_x. The dash box indicates the hours used to take the average. Times are in CST.
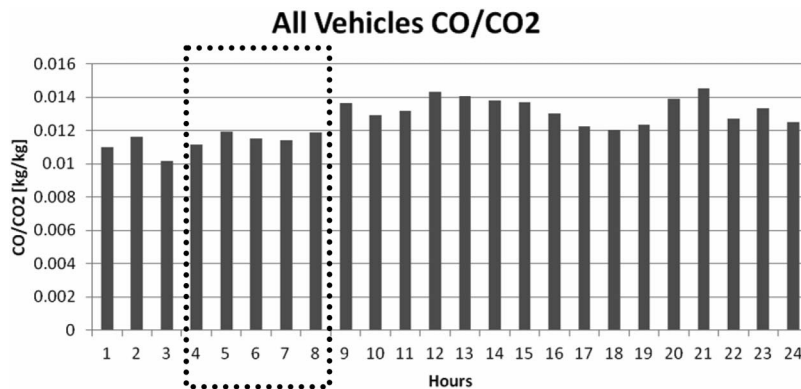

Figure 13. Diurnal variation of the CO/CO_2 ratio for the Galleria study site for September 28, 2009, as calculated by MOBILE6 and MOVES. The average of the early morning hours is 0.012 kg of CO per kg of CO_2. The dash box indicates the hours used to take the average. Times are in CST.
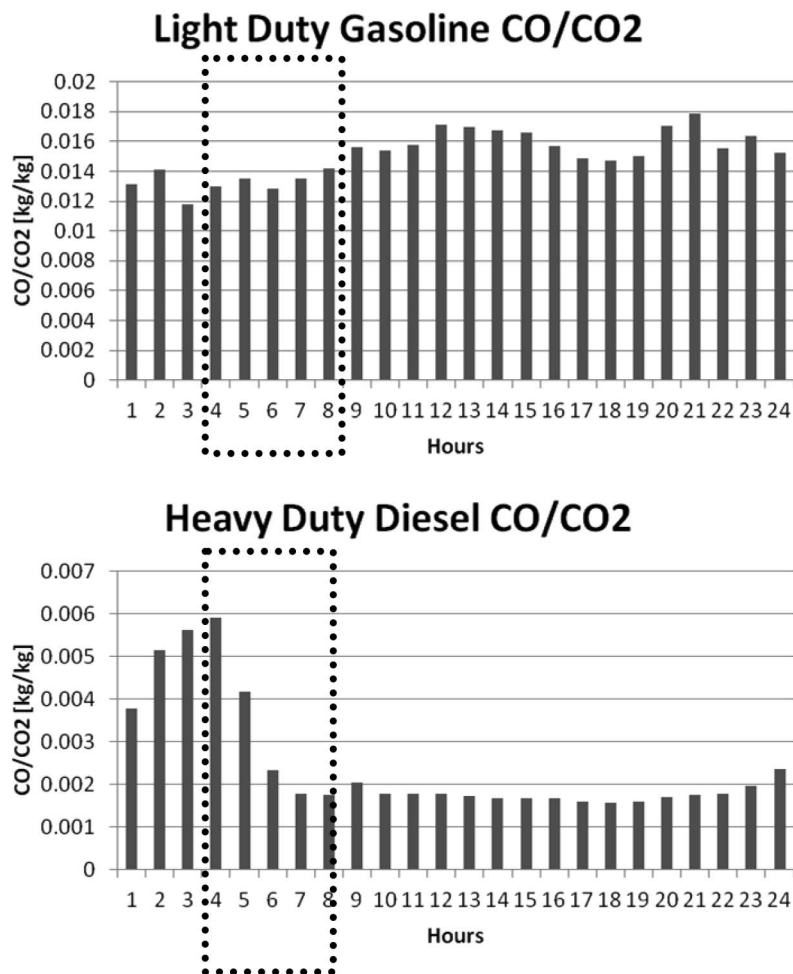
Light Duty Gasoline CO/CO2

Heavy Duty Diesel CO/CO2

Figure 14. Diurnal variation of CO/CO_2 ratio for light-duty gasoline and heavy-duty diesel vehicles calculated using MOVES. The average of the early morning hours is 0.013 kg of CO per kg of CO_2 and 0.0032 kg of CO per kg of CO_2, respectively. The dash box indicates the hours used to take the average. Times are in CST.

CO and NO/NO_x ratios. NO is emitted directly from vehicles and shows close relationship with CO ($r^2 = 0.91$ for all rush hour data, not shown). Table 5 also shows an excellent correlation of NO with NO_x ($r^2 = 0.96$). However the slope deviates from the 1:1 line and shows a value of 0.84 ppb_v NO/1 ppb_v NO_x. As NO_x is defined as the sum of NO and NO_2, the remaining NO_x emissions would be in form of NO_2, which is about 16% of the NO_x emissions, supporting our findings above again.

It may be possible that the MOVES model tends to underestimate NO_2 emissions, most likely from heavy-duty diesel. According to the EPA (2010b), the NO_2/NO_x emission ratio from gasoline driven vehicles rose from about 2.5% for car model years 1960–1980 to about 16% for car model years 1996 and younger. Relatively high NO_2/NO_x measured ratios of about 13% have also been found in recent studies (Villena et al., 2011), where diesel driven buses might have contributed significantly. Like that study, our study in particular included heavy-duty diesel trucks that frequented the highways. Generally, over the last decade and in particular in Europe, it has been observed than the NO_2 fraction of NO_x emitted from traffic has been rising (Carslaw, 2005; Carslaw et al., 2011;

Mavroidis and Chaloulaki, 2011). Grice et al. (2009) reported increases of the NO_2 fraction from 8.6% in 2000 to 12.4% in 2004 and predicted further average increases of the NO_2 fraction to 19.6% in 2010 and eventually 32% in 2020. The main reason for this increase is considered to be the use of diesel oxidation catalysts (DOCs) and catalyzed diesel particulate filters (DPFs) (Bar-Ilan et al., 2010; Bishop et al., 2010), which became standard equipment on new diesel trucks starting with 2007 (Ban-Weiss et al., 2008; see also: http://www.epa.gov/oms/highway-diesel/). These exhaust-treatment systems may enhance NO_2 fraction in NO_x emission up to 70% (Alvarez et al., 2008; Millstein and Harley, 2010).

The potential impact of diesel driven vehicles is further supported by the CO/CO_2 ratios shown in Table 5. The experimental data show overall CO/CO_2 molar emission ratios of 5.2 ± 0.3 ppb_v CO/1 ppm_v CO_2, which equals emission ratios of 0.0033 ± 0.0002 kg CO/kg CO_2. A similar magnitude was found for rush hour times in previous studies in Los Angeles (Newman et al., 2013). Rubio et al. (2010) and reference therein report CO/CO_2 emission ratios of 0.009 ± 0.005 kg CO/kg CO_2 as typical for catalytic cars and of 0.003 ± 0.001 kg CO/kg CO_2 as typical for

diesel powered vehicles. This supports the assumption that generally diesel vehicles exhibit lower CO/CO_2 emission ratios than gasoline driven vehicles. Unfortunately, there are no data available for September 28, 2009. However, it is plausible to assume that the VMT split on that day did not differ much from any other weekday included in the overall data set, and as a consequence the result would be very similar. The comparison with modeled calculations, as shown in Figure 13, shows that MOVES calculates 3 times higher CO/CO_2 than observed. As shown in Figure 14, it appears likely that MOVES overestimates the emission ratio of CO/CO_2 from light-duty gasoline vehicles because for heavy- and light-duty diesel vehicles the CO/CO_2 emission rates are close to the overall observed CO/CO_2 ratio, which is about an order of magnitude lower than for gasoline. The overestimation of the CO/CO_2 ratio is clearly related to the overestimation of CO from light-duty gasoline vehicles, as it was mentioned above for the overestimation of the CO/NO_x ratio.

Conclusion

During the time period July 15–October 15, 2009, continuous ambient air measurements were taken in the immediate vicinity of the Highway Junction I-59 South/610 located in the Galleria area, Houston. This study aimed at primary emissions of radical precursors such as HCHO and HONO from mobile sources and related species, and comparing these results with emission estimates from currently available emission models (MOBILE6 versus MOVES). The following main results were found:

(1) A CO versus NO_x ratio of around 6.01 $\pm$ 0.15 ppb$_v$ CO/1 ppb$_v$ NO_x ($r^2 = 0.91$) was found, which is in agreement with other studies (Parrish et al., 2009). Both MOBILE6 and MOVES overestimate the corresponding observed emission ratio. However, MOVES tends to get closer to the observed values, but is still 30% above the observed value.

(2) For HCHO/CO, an overall slope of 3.14 $\pm$ 0.14 g HCHO/kg CO was observed. Whereas MOBILE6 largely underestimates this ratio, MOVES calculates higher HCHO/CO ratios, but which are still lower than the observed one. MOVES shows surprisingly high HCHO/CO ratios during the early morning hours due to heavy-duty diesel "off-network" emissions such as emissions coming from idling and starting trucks. These emissions were underestimated in MOBILE6.

(3) The differences of the modeled CO/NO_x and HCHO/CO ratios are largely due to higher NO_x emissions in MOVES (30% increased from MOBILE6 for 2009) and higher HCHO emissions in MOVES (57% increased from MOBILE6 for 2009); CO emissions were about the same in both models.

(4) The observed HONO/NO_x emission ratio is around 0.017 $\pm$ 0.0009 kg HONO/kg NO_x, which is twice as high as is calculated in MOVES.

(5) The observed NO_2/NO_x emission ratio is around 0.16 $\pm$ 0.01 kg NO_2/kg NO_x, which is a bit more than 70% higher than the ratio calculated by MOVES.

(6) MOVES overestimates the CO/CO_2 emission ratio by a factor of 3 compared with the observations, which is 0.0033 $\pm$ 0.0002 kg CO/kg CO_2. This overestimation is coming from light-duty gasoline vehicles.

The above findings indicate that MOVES is performing better than MOBILE6. However, the findings suggest that the CO emissions are overestimated in MOVES, with this overestimation coming from light-duty gasoline vehicles. Fixing this overestimation could solve the problem of the underestimation of HCHO/CO and overestimation of CO/NO_x and CO/CO_2. Also, the findings suggest that emission ratios of HONO/NO_x and NO_2/NO_x from heavy-duty diesel are underestimated by MOVES, which attributes the same emission ratio for all vehicle types for HONO. We believe that these ratio underestimations come from underestimating the emissions of HONO and NO_2 from diesel vehicles, which are the main sources of these emissions. These species directly foster ozone formation.

Acknowledgment

References

Altshuller, A.P. 1993. Production of aldehydes as primary emissions and from secondary atmospheric reactions of alkenes and alkanes during the night and early morning hours. *Atmos. Environ.* 27A:21–32.

Alvarez, R., M. Weilenmann, and J.-Y. Favez. 2008. Evidence of increased mass fraction of NO_2 within real-world NO_x emissions of modern light vehicles—Derived from a reliable online measuring method. *Atmos. Environ.* 42:4699–4707. doi:10.1016/j.atmosenv.2008.01.046

Anderson, L.G., J.A. Lanning, R. Barrell, J. Miygishima, R.H. Jones, and P. Wolfe. 1996. Sources and sinks of formaldehyde and acetaldehyde: An analysis of Denver's ambient concentration data. *Atmos. Environ.* 30:2113–2123. doi:10.1016/1352-2310(95)00175-1

Ban-Weiss, G.A., J.P. McLaughlin, R.A. Harley, A.J. Kean, E. Grosjean, and D. Grosjean. 2008. Carbonyl and nitrogen dioxide emissions from gasoline- and diesel-powered motor vehicles. *Environ. Sci. Technol.* 42:3944–3950. doi:10.1021/es8002487

Bar-Ilan, A., J.R. Johnson, A. DenBleyker, L.-M. Chian, G. Yarwood, D. Hitchcock, and J.P. Pinto. 2010. Potential ozone impacts of excess NO_2 emissions from diesel particulate filters for on- and off-road diesel engines. *J. Air Waste Manage. Assoc.* 60:977–991. doi:10.3155/1047-3289.60.8.977

Bishop, G.A., A.M. Peddle, D.H. Stedman, and T. Zhan. 2010. On-road emission measurements of reactive nitrogen compounds from three California cities. *Environ. Sci. Technol.* 44:3616–3620. doi:10.1021/es903722p

Bishop, G.A., B.G. Schuchmann, D.H. Stedman, and D.R. Lawson. 2012. Multispecies remote sensing measurements of vehicle emissions on Sherman Way in Van Nuys, California. *J. Air Waste Manage. Assoc.* 62:1127–1133. doi:10.1080/10962247.2012.699015

Bishop, G.A., and D.H. Stedman. 1996. Measuring the emissions of passing cars. *Acc. Chem. Res.* 29:489–495. doi:10.1021/ar950240x

Byun, D., and K.L. Schere. 2006. Review of the governing equations, computational algorithms, and other components of the models—3 Community Multiscale Air Quality (CMAQ) modeling system. *Appl. Mech. Rev.* 59:51–77. doi:10.1115/1.2128636

Carslaw, D.C. 2005. Evidence of an increasing NO_2/NO_x emissions ratio from road traffic emissions. *Atmos. Environ.* 39:4793–4802. doi: 10.1016/j.atmosenv.2005.06.023

Carslaw, D.C., S.D. Beevers, J.E. Tate, E.J. Westmoreland and M.L. Williams. 2011. Recent evidence concerning higher NO_x emissions from passenger cars and light duty vehicles. *Atmos. Environ*. 39:167–177. doi: 10.1016/j.atmosenv.2011.09.063

Chen, J., S. So, H. Lee, M.P. Fraser, R.F. Curl, T. Harman, and F.K. Tittel. 2004. Atmospheric formaldehyde monitoring in the greater Houston area in 2002. *Appl. Spectrosc*. 58:243–247. doi:10.1366/000370204322843002

Czader, B.H., X. Li, and B. Rappenglueck. 2013. CMAQ modeling and analysis of radicals, radical precursors and chemical transformations. *J. Geophys. Res*. doi: 10.1002/jgrd.50807, posted online: 5 Sep 2013.

Czader, B.H., B. Rappenglück, P. Percell, D. Byun, F. Ngan, and S. Kim. 2012. Modeling nitrous acid and its impact on ozone and hydroxyl radical during the Texas Air Quality Study 2006. *Atmos. Chem. Phys*. 12:6939–6951. doi: 10.5194/acp-12-6939-2012

Dasgupta, P.K., J. Li, G. Zhang, W.T. Luke, W.A. McClenny, J. Stutz, and A. Fried. 2005. Summertime ambient formaldehyde in five U.S. metropolitan areas: Nashville, Atlanta, Houston, Philadelphia, and Tampa. *Environ. Sci. Technol*. 39:4767–4783. doi:10.1021/es048327d

Elshorbany, Y.F., R. Kurtenbach, P. Wiesen, E. Lissi, M. Rubio, G. Villena, E. Gramsch, A.R. Rickard, M.J. Pilling, and J. Kleffmann. 2009. Oxidation capacity of the city air of Santiago, Chile. *Atmos. Chem. Phys*. 9:2257–2273. doi:10.5194/acp-9-2257-2009

Franco, V., M. Kousoulidou, M. Muntean, L. Ntziachristos, S. Hausberger, and P. Dilara. 2013. Road vehicle emission factors development: A review. *Atmos. Environ*. 70:84–97. doi: 10.1016/j.atmosenv.2013.01.006

Fujita, E.M., D.E. Campbell, B. Zielinska, J.C. Chow, C.E. Lindhjem, A. DenBleyker, G.A. Bishop, B.G.Bishop, B.G. Schuchmann, D.H. Stedman, and D.R. Lawson. 2012. Comparison of the MOVES2010a, MOBILE6.2, and EMFAC2007 mobile source emission models with on-road traffic tunnel and remote sensing measurements. *J. Air Waste Manage. Assoc*. 62:1134–1149. doi:10.1080/10962247.2012.699016

Finlayson-Pitts, B. J., Wingen, L. M., Sumner, A. L., Syomin, D., and K.A. Ramazan. 2003. The heterogeneous hydrolysis of NO_2 in laboratory systems and in outdoor and indoor atmospheres and integrated mechanism. *Phys. Chem. Chem. Phys*. 5:223–242. doi:10.1039/b208564j

Grice, S., J. Stedman, A. Kent, M. Hobson, J. Norris, J. Abbott, and S. Cooke. 2009. Recent trends and projections of primary NO_2 emissions in Europe. *Atmos. Environ*. 43:2154–2167. doi:10.1016/j.atmosenv.2009.01.019

Houston-Galveston Area Council. 2009. H-GAC Conformity Determination—Appendix 5. http://www.h-gac.com/taq/airquality/conformity/2009/documents/Appendix5.pdf (accessed December 2012).

Kirchstetter, T. W., R.A. Harley, and D. Littlejohn. 1996. Measurement of nitrous acid in motor vehicle exhaust. *Environ. Sci. Technol*. 30:2843–2849. doi:10.1021/es960135y

Kleffmann, J., Becker, K. H., and P. Wiesen. 1998. Heterogeneous NO_2 conversion processes on acid surfaces: Possible atmospheric implications. *Atmos. Environ*. 32:2721–2729. doi:10.1016/S1352-2310(98)00065-X

Kleffmann, J., R. Kurtenbach, J.C. Lörzer, P. Wiesen, N. Kalthoff, N. Vogel, and B. Vogel. 2003. Measured and simulated vertical profiles of nitrous acid. Part I: Field measurements. *Atmos Environ*. 37:2949–2955. doi:10.1016/S1352-2310(03)00242-5

Klemp, D., K. Mannschreck, H.W. Pätz, M. Habram, P. Matuska, and F. Slemr. 2002. Determination of anthropogenic emission ratios in the Augsburg area from concentration ratios: Results from long-term measurements. *Atmos Environ*. 36:S61–S80. doi:10.1016/S1352-2310(02)00210-8

Kota, S.H., Q. Ying, Q., and G.W. Schade. 2012. MOVES versus MOBILE6.2: Differences in emission factors and regional air quality predictions. Paper presented at Transportation Research Board 91st Annual Meeting, Washington DC, January 22–26, 2012, paper 12-4438.

Kurtenbach, R., K.H. Becker, J.A.G. Gomes, J. Kleffmann, J.C. Lörzer, M. Spittler, P. Wiesen, R. Ackermann, A. Geyer, and U. Platt. 2001. Investigations of emissions and heterogeneous formation of HONO in a road traffic tunnel. *Atmos. Environ*. 35:3385–3394. doi:10.1016/S1352-2310(01)00138-8

Lammel, G., and J.N. Cape. 1996. Nitrous acid in the atmosphere. *Chem. Soc. Rev*. 9:361–369. doi:10.1039/cs9962500361

Lefer, B., and B. Rappenglück. 2010. The TexAQS-II radical and aerosol measurement project (TRAMP). *Atmos. Environ*. 44:3997–4004. doi: 10.1016/j.atmosenv.2010.05.053

Leuchner, M., and B. Rappenglück B. 2010. VOC source–receptor relationships in Houston during TexAQS-II. *Atmos. Environ*. 44:4056–4067. doi: 10.1016/j.atmosenv.2009.02.029

Luke, W.T., P. Kelley, B.L. Lefer, J. Flynn, B. Rappenglück, M. Leuchner, J.E. Dibb, L.D. Ziemba, C.H. Anderson, and M. Buhr. 2010. Measurements of primary trace gases and NO_y composition in Houston, Texas. *Atmos. Environ*. 44:4068–4080. doi: 10.1016/j.atmosenv.2009.08.014

Mao, J., X. Ren, S. Chen, W.H. Brune, Z. Chen, M. Martinez, H. Harder, B. Lefer, B. Rappenglück, J. Flynn, and M. Leuchner. 2010. Atmospheric oxidation capacity in the summer of Houston 2006: Comparison with summer measurements in other metropolitan studies. *Atmos. Environ*. 44:4107–4115. doi: 10.1016/j.atmosenv.2009.01.013

Mavroidis, I., and A, Chaloulaki. 2011. Long-term trends of primary and secondary NO_2 production in the Athens area. Variation of the NO_2/NO_x ratio. *Atmos. Environ*. 45:6872–6879. doi: 10.1016/j.atmosenv.2010.11.006

McGaughey, G.R., N.R. Desai, D.T. Allen, R.L. Seila, W.A. Lonneman, M.P. Fraser, R.A. Harley, A.K. Pollack, J.M. Ivy, and J.H. Price. 2004. Analysis of motor vehicle emissions in a Houston tunnel during the Texas Air Quality Study 2000. *Atmos. Environ*. 38:3363–3372. doi:10.1016/j.atmosenv.2004.03.006

Millstein, D.E., and R.A. Harley. 2010. Effects of retrofitting emission control systems on in-use heavy diesel vehicles. *Environ. Sci. Technol*. 44:5042–5048. doi:10.1021/es1006669

Morris, G.A., B. Ford, B. Rappenglück, A.M. Thompson, A. Mefferd, F. Ngan, and B. Lefer. 2010. An evaluation of the influence of the morning residual layer on afternoon ozone concentrations in Houston using ozonesonde data. *Atmos. Environ*. 44:4024–4034. doi: 10.1016/j.atmosenv.2009.06.057

Newman, S., S. Jeong, M.L. Fischer, X. Xu, C.L. Haman, B. Lefer, S. Alvarez, B. Rappenglueck, E.A. Kort, A.E. Andrews, J. Peischl, K.R. Gurney, C.E. Miller, and Y.L. Yung. 2013. Diurnal tracking of anthropogenic CO_2 emissions in the Los Angeles basin megacity during spring, 2010. *Atmos. Chem. Phys*. 13:4359–4372. doi: 10.5194/acp-13-4359-2013

Olaguer, E.P., C.E. Kolb, B. Lefer, B. Rappenglück, R. Zhang, and J.P. Pinto. 2013. Overview of the SHARP campaign: Motivation, design, and major outcomes. *J. Geophys. Res*. in press.

Parrish, D.D., D.T. Allen, T.S. Bates, M. Estes, F.C. Fehsenfeld, G. Feingold, R. Ferrare, R.M. Hardesty, J.F. Meagher, J.W. Nielson-Gammon, R.B. Pierce, T.B. Ryerson, J.H. Seinfeld, and E.J. Williams. 2009. Overview of the Second Texas Air Quality Study (TexAQS II) and the Gulf of Mexico Atmospheric Composition and Climate Study (GoMACCS). *J. Geophys. Res*. 114:1–28. doi: 10.1029/2009JD011842

Rappenglück, B., P.K. Dasgupta, M. Leuchner, Q. Li, and W. Luke. 2010. Formaldehyde and its relation to CO, PAN, and SO_2 in the Houston-Galveston airshed. *Atmos. Chem. Phys*. 10:2413–2424. doi:10.5194/acp-10-2413-2010

Rappenglück, B., R. Perna, S. Zhong, and G.A. Morris. 2008. An analysis of the vertical structure of the atmosphere and the upper-level meteorology and their impact on surface ozone levels in Houston, Texas. *J. Geophys. Res*. 113: D17315. doi: 10.1029/2007JD009745

Rappenglück, B., R. Schmitz, M. Bauerfeind, F. Cereceda-Balic, D. v. Baer, D., H. Jorquera, Y. Silva, and P. Oyola. 2005 An urban photochemistry study in Santiago de Chile. *Atmos. Environ*. 39:2913–2931. doi:10.1016/j.atmosenv.2004.12.049

Rubio, M.A., I. Fuenzalida, E. Salinas, E. Lissi, R. Kurtenbach, and P. Wiesen. 2010. Carbon monoxide and carbon dioxide concentrations in Santiago de Chile associated with traffic emissions. *Environ. Monit. Assess*. 162:209–217. doi: 10.1007/s10661-009-0789-9

Sarwar, G., S.J. Roselle, R. Mathur, W. Appel, R.L. Dennis, and B. Vogel. 2008. A comparison of CMAQ HONO predictions with observations from the Northeast Oxidant and Particle Study. *Atmos Environ*. 42:5760–5770. doi:10.1016/j.atmosenv.2007.12.065

Texas Department of Transportation. 2009a. 2009 Houston District Traffic Map. http://ftp.dot.state.tx.us/pub/txdot-info/tpp/traffic_counts/2009/hou_base.pdf (accessed December 2012).

Texas Department of Transportation. 2009b. Texas Transportation Institute Emission Inventory Utilities User's Guide, July 2009. College Station, TX: Texas Transporation Institute, The Texas A&M University System.

Texas Department of Transportation. 2011. Texas Transportation Institute Inventory Estimation Utilities Using MOVES: MOVESUTL User's Guide, August 2011.ftp://amdaftp.tceq.texas.gov/pub/Mobile_EI/MOVES/Utilities/MOVES_Utilities_ Update_FY11_Report.pdf (accessed December 2012).

U.S. Environmental Protection Agency. 2003. EPA MOBILE6.2 User's Guide, August 2003. http://www.epa.gov/oms/models/mobile6/420r03010.pdf. (accessed December 2012).

U.S. Environmental Protection Agency. 2010a. EPA Motor Vehicle Emission Simulator (MOVES) User Guide for MOVES2010a, August 2010. http://www.epa.gov/oms/models/moves/MOVES2010a/420b10036.pdf. (accessed December 2012).

U.S. Environmental Protection Agency. 2010b. Development of Emission Rates for the MOVES Model. Sierra Research for US EPA, March 3, 2010. http://www.epa.gov/oms/models/moves/documents/420r12022.pdf. (accessed December 2012).

U.S. Environmental Protection Agency. 2011. US EPA Heavy-Duty Vehicle Greenhouse Gas (HDGHG) Emissions Inventory for Air Quality Modeling Technical Support Document, August 2011. http://www.epa.gov/otaq/climate/documents/420r11008.pdf. (accessed December 2012).

U.S. Environmental Protection Agency. 2012. EPA Motor Vehicle Emission Simulator (MOVES) User Guide for MOVES2010b, June 2012. http://www.epa.gov/otaq/models/moves/documents/420b12001b.pdf.   (accessed December 2012).

Vallamsundar, S., and J. Lin. 2011. MOVES Versus MOBILE—Comparison of greenhouse gas and criterion pollutant emissions. *Transport. Res. Rec.* 2233:27–35. doi: 10.3141/2233-04

Villena, G., J. Kleffman, R. Kurtenbach, P. Wiesen, E. Lissi, M.A. Rubio, G. Croxatto, and B. Rappenglück. 2011. Vertical gradients of HONO, NO$_x$ and O$_3$ in Santiago de Chile. *Atmos. Environ.* 45:3867–3873. doi: 10.1016/j.atmosenv.2011.01.073

Wallace, H.W., B.T. Jobson, M.H. Erickson, J.K. McCoskey, T.M. VanReken, B.K. Lamb, J.K. Vaughan, R.J. Hardy, J.I. Cole, S.M. Strachan, and W. Zhang. 2012. Comparison of wintertime CO to NO$_x$ ratios to MOVES and MOBILE6.2 on-road emissions inventories. *Atmos Environ.* 63:289–297. doi:10.1016/j.atmosenv.2012.08.062

Ziemba, L.D. J.E. Dibb, R.J. Griffin, C.H. Anderson, S.I. Whitlow, B.L. Lefer, B. Rappenglück, B., and J. Flynn. 2010. Heterogeneous conversion of nitric acid to nitrous acid on the surface of primary organic aerosol in an urban atmosphere. *Atmos. Environ.* 44:4081–89. doi: 10.1016/j.atmosenv.2008.12.024

Zweidinger, R.B., J.E. Sigsby, S.B. Tejada, F.D. Stump, D.L. Dropkin, W.D. Ray, and J.W. Duncan. 1988. Detailed hydrocarbon and aldehyde mobile source emissions from roadway studies. *Environ. Sci. Technol.* 22:956–962. doi:10.1021/es00173a015

About the Authors

Bernhard Rappenglück is an associate professor in atmospheric science at the Department of Earth and Atmospheric Sciences, University of Houston, Houston, Texas.

Graciela Lubertino is a Chief Air Quality Planner at the Houston-Galveston Area Council, Houston, Texas.

Sergio Alvarez is a Researcher II, **Julia Golovko** and **Beata Czader** are postdoctoral fellows, and **Luis Ackermann** is a Researcher I at the Department of Earth and Atmospheric Sciences, University of Houston, Houston, Texas.